EPJ Web of Conferences **24**, 06003 (2012)
DOI: 10.1051/epjconf/20122406003

Radon potential mapping in Piemonte (North-West Italy): An experimental approach

E. Chiaberto, M. Magnoni, E. Serena, S. Procopio, A. Prandstatter and F. Righino

ARPA Piemonte, Dipartimento Radiazioni - Via Jervis, 30
10015 Ivrea (TO), Italy

1 Introduction

Early radon studies in Piemonte, an administrative district in North-West Italy (25200 km^{-2}, around 4300000 inhabitants) have been done since 1990-1991, when a general radon survey of the dwellings of Piemonte was performed in order to assess the average radon exposure of the whole population. The survey, executed in the framework of the National Radon Survey by the National Environmental Protection Agency (former ANPA, now ISPRA) and ISS (National Health Institute), involved about 430 dwellings, chosen randomly with a stratified sampling technique.

After this first step, radon researches were continued in different areas of Piemonte and involved schools as well as dwellings.

In particular, radon surveys were conducted in areas where the geological conditions (*i.e.*, the occurrence of rocks with Uranium content well above the typical average concentration found in the Earth crust) appear to favour a stronger radon emanation. Besides this kind of studies, other surveys were performed in order to assess the radon exposure in schools, where children and young students, the most radio-sensitive part of the population could be exposed to high radon concentrations.

These extensive radon monitoring programs led to the implementation of

a large radon database of more than 3500 radon measurements distributed all over the Piemonte Region. The whole radon database, before being used as a tool for the definition of the radon prone areas of Piemonte, was subject to a careful analysis and selection, in order to eliminate not representative measurements. In particular, to minimize a possible bias due to the well-known radon fluctuations both on daily and seasonal basis, we considered only long term measurements (annual), performed using the nuclear track etch detectors technique (LR 115 or CR-39).

The radon potential mapping of the whole Piemonte was then achieved developing a "geolithological correlation model", based on a statistical analysis of the radon experimental data and the underlying geological, lithological and radiometric characteristics of soils and rocks.

2 Material and methods

The well-known phenomenon of the fluctuation of indoor radon concentrations both on daily and seasonal basis is probably the most important factor to be taken into account in order to harmonize a radon database. In fact, grab sampling measurements and short-term measurements (*i.e.*, lasting a few days) often give results very different from long-term measurements, that are considered much more reliable, especially for radon mapping purposes. Therefore, for each sampling site, we decided to consider only those measurements able to give the annual average radon concentration.

Moreover, in order to minimize possible calibration and measurement procedure bias, we decided to include only the measurements performed with the same technique, based on a dosimeter equipped with standard nuclear track etch detectors (LR 115 or CR-39). In this way, the original database was resized to about 2400 measurements.

In order to reduce the heterogeneity of the sample, due in particular to the floor where the dosimeters were installed (fig. 1), a ground floor normalization of the data referred to higher floors was performed and validated (fig. 2).

Assuming that the distribution of the indoor radon concentration at ground floor is approximately lognormal, the normalization was done as follows:

$$f(C_{GF}) = \frac{1}{\sqrt{2\pi}\sigma_{GF}} \frac{e^{-\frac{(\ln(C_{GF})-\mu_{GF})^2}{2{\sigma_{GF}}^2}}}{C_{GF}}$$

with $\mu_{GF} = \ln(GM_{GF})$, $\sigma_{GF} = \ln(GSD_{GF})$, the GM_{GF} and GSD_{GF} being

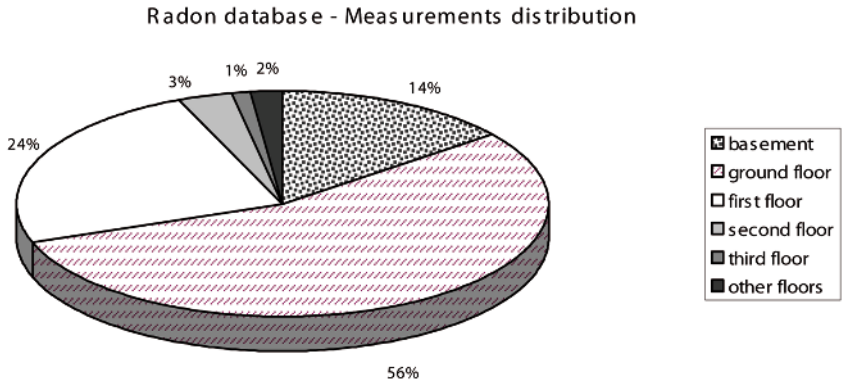

Figure 1: Radon measurements available in our database: 56% were performed at ground floor.

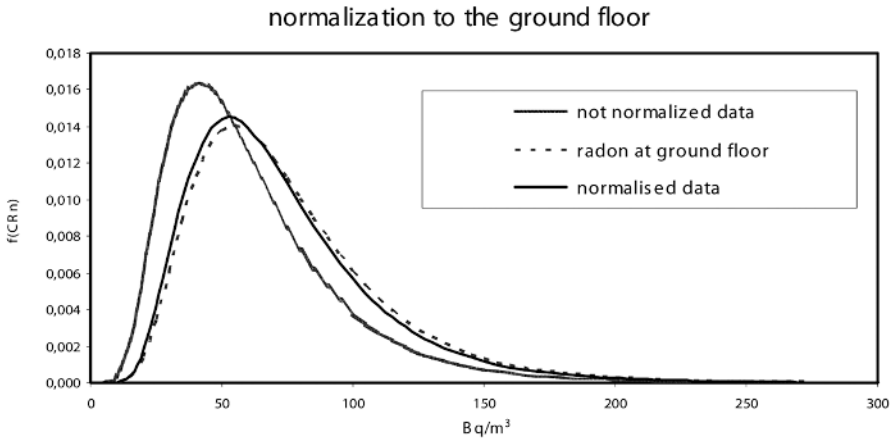

Figure 2: Normalization to ground floor.

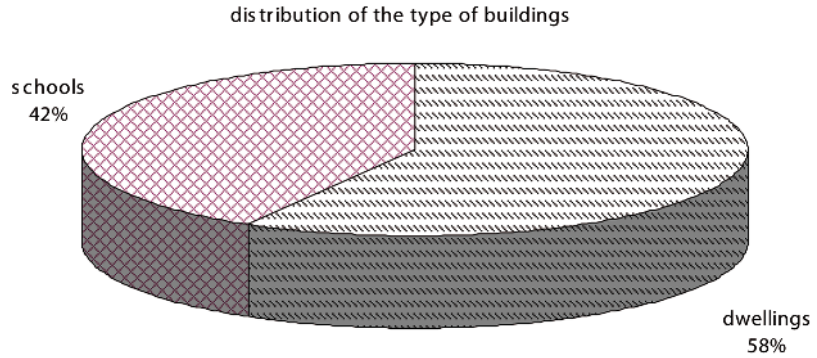

Figure 3: Schools represent 42% of the whole radon database.

the geometric mean and geometric standard deviation. If we suppose that, in any given dwelling, a linear relationship holds between the radon concentration at ground floor (C_{GF}) and the radon concentration C_F at a generic floor F, *i.e.*:

$$C_F = kC_{GF},$$

where k is a constant to be determined, the radon distribution at generic floor F can be written as follows:

$$f(C_F) = \frac{1}{\sqrt{2\pi}\sigma_F} \frac{e^{-\frac{(\log(C_F)-\mu_F)^2}{2{\sigma_F}^2}}}{C_F},$$

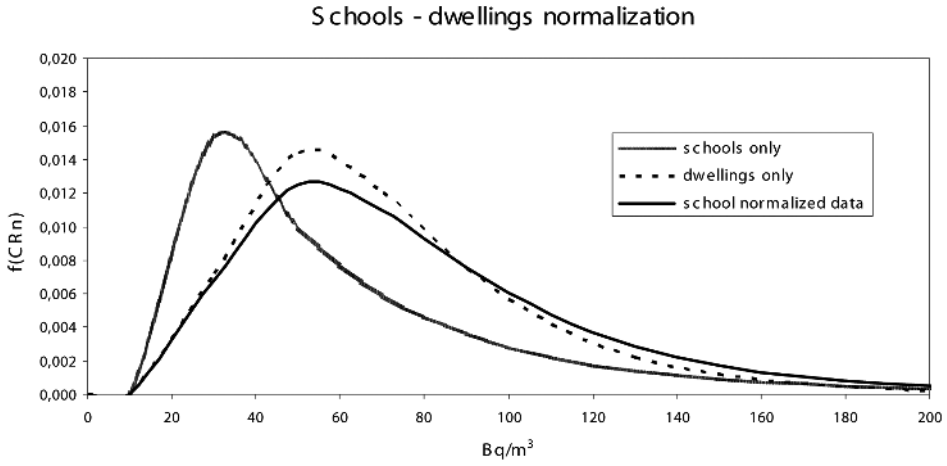

Figure 4: Normalization from schools to dwellings.

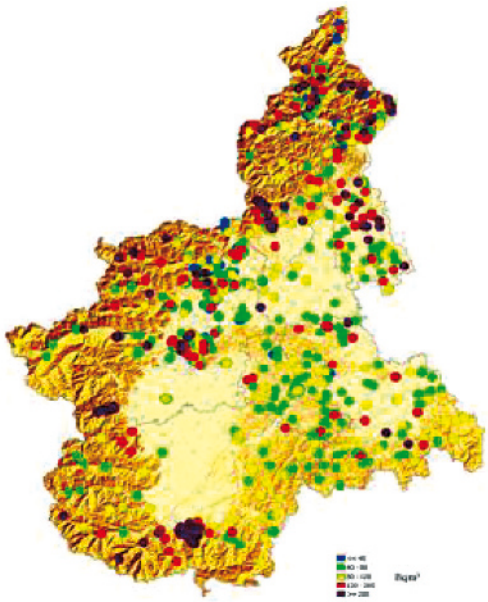

Figure 5: The radon experimental data (normalized to ground floor).

where $\mu_F = \ln k + \mu_{GF}$, $\sigma_F = \sigma_{GF}$ and k is given by $k = \frac{e^{\mu_F}}{e^{\mu_{GF}}}$.

In order to include also the measurements performed in schools that represent the 42% of the whole database (fig. 3), another normalization is needed. In fact, because of the different constructive characteristics, the radon concentration in typical school buildings is generally lower than those in dwellings. Therefore, the "school concentrations" were normalized to "dwelling concentrations": $C_{dwellings} = C_{schools} + \Delta C$, where $\Delta C = GM_{dwellings} - GM_{schools}$ (fig. 4).

Once obtained a global ground floor normalized database, the following step was the definition of the basic criteria of the radon potential mapping. First of all it was decided to consider a subdivision of the Region in 1206 administrative units, corresponding to the municipality of Piemonte. It was then defined, as radon potential indicator, the mean of the radon concentration measurements performed at ground floor and the related log-normal distribution. Unfortunately, being the number of municipality of Piemonte very large (1206), the actual database cannot give a representative sample for each administrative district. In fact, only in the municipality where the number of valid measurements were greater than 4, the mean and the related log-normal distribution was experimentally obtained. Therefore, in order to attribute an appropriate mean radon concentration value and a

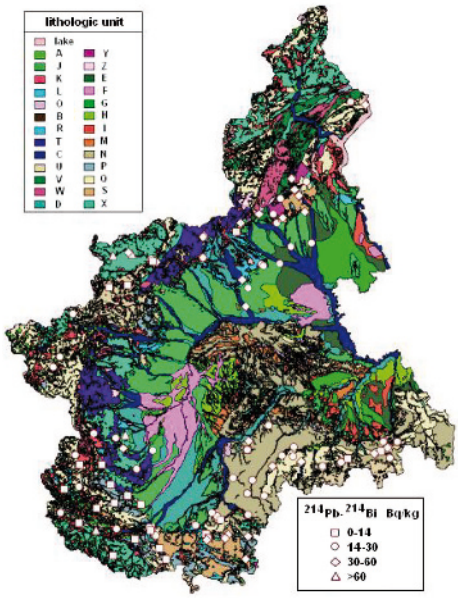

Figure 6: Lithological and radiometric characteristics of soils and rocks.

reliable log-normal distribution to all the administrative districts, we had to estimate these quantities for the municipalities where the experimental data are lacking. So, a "geolithological correlation model" was developed, based on a statistical analysis of the radon experimental data (fig. 5) and the underlying geological, lithological (fig. 6) and radiometric characteristics of the soils and rocks.

An *ad hoc* subdivision of the Region in lithological-radiometric units was performed taking into account also for the results of the analysis of a wide measurement campaign (γ spectrometry) of the natural radioactivity (mainly due to uranium) in the soils and the rocks of Piemonte.

In table I are reported the data of ^{214}Pb and ^{214}Bi, the natural radioisotopes belonging to the uranium series that, being the short lived radon daughters, can be regarded as good indicators of the potential radon emanation.

The rocks were then classified in four different categories, accordingly with their radioactivity content (average values of ^{214}Pb and ^{214}Bi):

very low radioactivity (< 14 Bq/kg)
low radioactivity (14 Bq/kg -30 Bq/kg)
high radioactivity (30 Bq/kg - 60 Bq/kg)
very high radioactivity (> 60 Bq/kg).

Table I: γ-spectrometry measurements (HPGe) in various types of soils and rocks (^{214}Pb e ^{214}Bi).

Soil	Locality	^{214}Pb ($\mathrm{Bq\,kg^{-1}}$)	^{214}Bi ($\mathrm{Bq\,kg^{-1}}$)
porphyritic granite	Campiglia Cervo	91.9	104.7
augen gneiss	Noasca	73.4	66.6
augen gneiss	Ceresole Reale	68.0	61.8
porphyroid and uranium minerals	Canosio, Preit	396850	359350
porphyroid	Canosio	8986	8096
volcanic rock	Masserano	62.9	56.5
gneiss	Vinadio	165.5	149.7
gneiss	Barge	96.1	83.1
biotitic diorite	Netro	37.9	34.2
alluvial cone gravel	Scopello	35.9	34.4
pebble	Sordevolo	32.5	30.5
sandstone	Roccaverano	32.8	28.6
alluvium	Borgosesia	35.6	32.3
alluvium	Quarona	42.5	40.0
alluvium	Livorno Ferraris	37.1	38.4
alluvium	Saluggia	38.1	35.5
porphyry	Serravalle Sesia	36.3	33.2
calcareous and micaceous schist	Limone Piemonte	31.5	34.4
orthogneiss	Pamparato	29.9	33.9
micaschist	Pamparato	28.5	31.6
micaceous quartz schist	Pamparato	52.0	48.3
quartz porphyry	Frabosa Soprana	37.6	37.9
albite gneiss	Locana	61.7	57.2
pink granite	Vidracco	48.0	44.8
augen gneiss	Noasca	46.3	42.6
silty marl	Tornese	39.5	35.8
polygenic conglomerates	Bagnasco	33.4	31.0
quartz schist	Garessio	38.6	33.9
clay marl	Cortemilia	34.4	30.2
clay marl	Diano d' Alba	31.5	29.3
marl	Alba	44.1	40.6
serpentinite	Vidracco	60.4	55.0
diorite	Traversella	39.9	35.3
biotitic gneiss	Traversella	58.7	51.7
silty marl	Carrosio	37.5	25.9
schist \ gneiss	Cannobio	37.5	32.9
silty marl	Tornese	37.0	29.3
gneiss	San Front	35.1	28.7
marl	Castagnole delle Lanze	26.4	24.4
sandstone	Vesime	24.0	22.9
clay marl	Monastero Bormida	24.8	28.7

Table I: Continued.

granite	Valle San Nicolao	20.0	22.2
biotite micaschist	Valduggia	24.1	26.1
clay marl	Bubbio	26.7	24.1
biotic granite	Pray	30.8	29.1
black clay	Cavaglià	27.7	24.2
clay	Cavaglià	21.7	22.0
alluvium	Carisio	21.3	19.4
alluvium	Bronzo	17.5	16.1
fluvioglacial gravel	Arborio	30.6	27.4
reddish paleosol	Cigliano	15.9	16.7
quartz porphyry	Brusnengo	25.2	25.0
quartz schist	Robilante	27.9	25.7
quartz schist	Robilante	26.5	24.9
chlorite-bearing granite	Valdieri	17.8	19.7
calcareous and micaceous schist	Borgo San Dalmazzo	23.4	22.0
ottrelite schist	Frabosa Sottana	23.3	21.8
marly sandstone	Vicoforte di Mondovì	21.8	24.8
marly sandstone	Vicoforte di Mondovì	28.1	26.6
sandy marl	Mondovì	19.7	17.6
dolomitic limestone	Villanova di Nondovì	25.0	27.2
micaschist	Frabosa Soprana	20.1	19.2
amphibolite	Locana	20.2	18.3
silty marl	Arquata Scrivia	28.3	24.7
clay marl	Grondona	30.8	29.0
silt	Gavi	25.8	23.8
silty marl	Ponzone	27.1	25.0
dolomite and limestone	Voltaggio	25.3	22.2
silty marl and silt	Cassinelle	27.6	24.5
sandstone	Dogliani	19.8	18.2
gray marl	Murazzano	27.9	25.6
gray sandstone	Murazzano	15.6	14.3
yellow sand	Murazzano	19.6	16.9
gray sandstone	Bossolasco	17.2	15.6
grey sand	Bossolasco	21.1	20.4
sandstone	Cortemilia	21.3	19.0
marl	Ceva	29.0	25.5
sandstone	Monesiglio	18.7	17.5
grey marl	Monesiglio	18.3	16.9
yellow sand	Diano d' Alba	19.7	17.5
fine-grained gneiss (Gneiss minuti complex)	Cavaglio Spoccia	30.3	25.7
silty marl, silt and sandstone	Arquata Scrivia	30.9	23.5
silty marl	Cassinelle	20.0	17.3
dolomite and limestone	Voltaggio	23.8	22.3
sandy marl, silt and sandstone	Ponzone	17.8	15.4

Table I: Continued.

silt and sandstone	Gavi	19.3	13.1
calcareous schist	Pragelato	29.1	25.8
calcareous schist	Novalesa	31.4	26.1
calcareous schist	Sestriere	27.1	19.8
gneiss \ micaschist	Venasca	22.3	20.6
gneiss \ micaschist	Saluzzo	32.0	26.2
marble	Argentera	23.6	21.2
calcareous schist	Pontechianale	18.7	16.3
calcareous schist	Capoluogo	30.1	24.9
phyllitic carbonate schist	Prazzo	18.9	16.6
gneiss \ micaschist	Paesana	22.2	11.9
gneiss	Demonte	18.2	15.5
melanocratic diorite	Netro	2.0	2.4
dolomitic limestone	Borgo S. Dalmazzo	6.0	6.6
micaceous limestone	Limone Piemonte	10.9	10.3
micaceous limestone	Roccavione	3.7	4.3
biotite gneiss	Valdieri	13.8	13.3
quartzite	Frabosa Sottana	12.6	13.9
dolomitic limestone	Vernante	12.9	12.8
limestone	Valdieri	5.4	5.3
sandy conglomerate	Vicoforte	11.6	10.4
quartz conglomerate	Frabosa Soprana	7.4	7.0
quartzite sandstone	Frabosa Soprana	6.5	5.6
amphibolite	Locana	0.8	0.3
pyroxenite	Balme	1.4	1.2
serpentine schist	Ala di Stura	0.3	0.3
silty marl, sandstone and silt	Carrossio	14.6	12.6
calcarenite	Bosio	14.2	13.0
sandstone, sandy marl, silt	Molare	10.3	9.4
sandstone	Diano d'Alba	13.2	12.5
sandstone	Molare	11.9	10.6
polygenic conglomerate	Bosio	12.7	10.9
micaschist	Caraglio	10.4	9.5
gneiss, micaschist	Sampeyre	9.6	8.5
serpentinite	Acceglio	1.5	1.6
marble	Pradleves	12.9	12.6
marble	Sambuco	3.2	2.8
marble	San Damiano Macra	10.2	9.4
serpentinite	Casteldelfino	0.9	1.0
limestone - dolomite breccia	Dronero	7.1	6.3
marble	Castelmagno	10.1	7.7

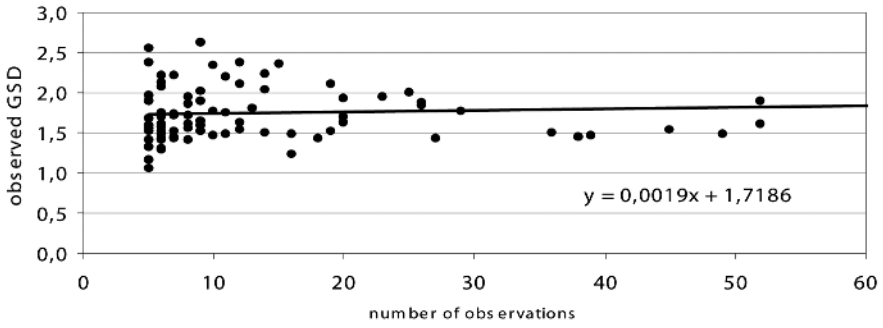

Figure 7: Observed geometric standard deviation.

Taking into account for this information, it was possible to establish a more simple subdivision of the Region in only 26 lithological-radiometric units, instead of the original 44 lithological units (fig. 6). Radon was then evaluated, using the experimental radon concentrations, in each of the new 26 lithological-radiometric units, thus obtaining, for each unit, a "Lithologic Mean" (LM)(table II).

It was then possible to compute the radon concentration mean AM_j for the generic $j^{\text{-th}}$ municipality in whose area p different lithological-radiometric units were present:

$$AM_j = \sum_{k=1}^{p} \frac{AL_k \cap AC_j}{AC_j} \cdot LM_k, \tag{1}$$

where:
LM_k: Rn concentration mean (normalized to ground floor) of the $k^{\text{-th}}$ lithological unit
AC_j: surface of the $j^{\text{-th}}$ municipality area
AL_k: surface of the $k^{\text{-th}}$ lithological unit

The geometric standard deviation (GSD), necessary for the definition of the log-normal distributions, was evaluated considering the asymptotic value of all the experimental GSDs (fig. 7).

This approach was then validated comparing the values predicted by the model with the means experimentally calculated in those municipalities where the data were available (fig. 8). In this analysis, in order to avoid auto-correlation effects, the lithological means used for the model prediction were calculated excluding the data of the municipality where the mean was evaluated from experimental data.

Table II: Lithological-radiometric units.

Lito code	**New lithologic units**	**LM** $\mathbf{Bq\,m^{-3}}$
A	Talus slopes, debris cones and alluvial fans	129
B	Peat and swamp deposits of recent lakes	27
C	Gravel – recent and present river beds	159
D	Terraced gravelly, sandy and silty alluvial deposits	72
E	Pebbly coarse sandy and silty alluvial deposits	85
F	Predominantly sandy alluvial deposits	90
G	Mildly weathered silty and sandy alluvial deposits	98
H	Predominantly silty and clayey alluvial deposits with sand-gravelly lenses and clayey loess; *"ferretto"*	73
I	Alternating reddish gravelly and sandy alluvial deposits and yellow sand with frequent clay, weathered caolinicclays	133
J	Fluvioglacial gravel and pebble alluvial deposits, with large boulders, weathered forming clay soils ("ferretto")	97
K	Recent moraines without significant weathering	149
L	Moraine deposits with strongly weathered cobbles ("ferretto" weathering)	82
M	Silty clay with interbedded sands; marl and clay with sand. Clays	97
N	Sands, coarse sands, with gravel lenses and intercalating to sandstones and marls, Poorly cemented calcarenites and calcirudites Marly calcarenites and marly limestones interbedded with limited limestones, silty marls and sandstones Polygenic conglomerates, conglomerates and sandstones forming thick layers with intercalating sandy marls, clay and limestone Alternating limestones, marly limestones, calcareous sandstones, clays and marls Sandy and silty marls and clay marls, marl with alternating sandstones and limestones, marly limestones and clays	64
O	Clays and marly clays with lenses of gypsum and subordinate intercalations of vacuolar limestone, sand or sandstone ("gessoso-solfifera" formation), Vacuolar dolomites and vacuolar limestones	75
P	Gypsum deposits Medium-thin layered limestones, marly limestones, cherty limestones massive or thickly-layered limestones Dolomite and dolomitic limestones with interbedded graphite-micaschists and lenses of granite. Peridotite and lherzolite. Saccharoid, frequently silicate marbles, dolomitic marbles	123
Q	Flysch successions and their metamorphic derivates: clays, marls, sandstones, limestones, marly limestones; calcareous schists, micaschist, gneiss, slates	88
R	Quartzites, quartzarenites, sandy and conglomeratic quartzites, micaceous quartzites, quartz schists	82
S	Sericitic schists and sericitic quartz schist. Porphyrites and weathered porphyrites. Rhyolites, rhyolitic tuffs and agglomerates Andesites, andesitic tuffs and tuffaceous agglomerates	229

Table II: Continued.

T	Micaschists gneiss, quartz-micaschists phyllitic micaschists	169
U	Amphibolites, serpentinites, prasinites	129
V	Kinzigite and amphibolite gneiss, associated augen gneiss	97
W	Basic granulites and associated amphibolites, melanocratic diorites, diabase and metagabbros	96
X	Tabular augen gneiss, with closely spaced joints, fine-grained gneiss, augen gneiss, massive granitic gneiss with widely spaced joints, porphyroids White, green, pink massive granite with no cover and weathering. Aplites and pegmatites	123
Y	Weathered granites and deriving thick arcosic sands	62
Z	Syenite, monzonite, quartzdiorite, granodiorite	913

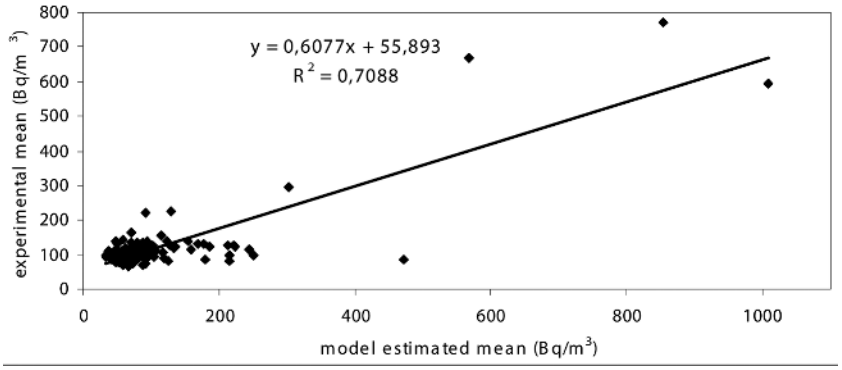

Figure 8: Validation of the model.

The result obtained in this validation analysis can be considered quite good ($R^2 = 0.71$), thus allowing the use of the model for prediction purposes.

3 Results and discussion

It is well-known that the experimental data of indoor radon can be considered roughly distributed accordingly to a log-normal function:

$$f(c) = \frac{e^{\frac{-(\ln c-\mu)^2}{2\sigma^2}}}{\sqrt{2\pi}\cdot\sigma\cdot c} \tag{2}$$

where

$$\mu = \frac{1}{n}\sum_{i=1}^{n}\ln(c_i) \quad \sigma = \sqrt{\frac{1}{n-1}\sum_{i=1}^{n}[\ln(c_i)-\mu]^2} \tag{3}$$

and c_i are the experimental values of the radon concentration.

The radon mapping of Piemonte was thus performed defining, for each municipality, the function $f(c)$ reported in eq. (2), whose parameters were calculated in two different ways. For the municipality where experimental data were considered representative, $f(c)$ was defined simply evaluating μ and σ from eq. (3). In the other cases, σ was calculated from the extrapolation of the experimental GSDs (see fig. 7), while μ was calculated from the AM_j, evaluated by means of eq. (1), taking into account that the arithmetic mean AM of a variable log-normally distributed can be expressed as follows:

$$AM = \int_0^\infty \frac{e^{\frac{-(\ln x-\mu)^2}{2\sigma^2}}}{\sqrt{2\pi}\cdot\sigma}\mathrm{d}x = e^{\mu+\frac{\sigma^2}{2}}. \tag{4}$$

From the log-normal distributions, can also be calculated, in each sampling unit, the percentage of dwellings that exceed a given reference level R_L .

$$P_{\%RL} = 100\cdot\int_{R_L}^\infty \frac{e^{\frac{-(\ln c-\mu)^2}{2\sigma^2}}}{\sqrt{2\pi}\cdot\sigma\cdot c}\mathrm{d}c. \tag{5}$$

In fig. 9 the results of the calculation of eq. (5) for the whole Region are reported. It can be seen that about 2% of the dwellings of Piemonte exceed the European Reference level of $200\,\mathrm{Bq\,m^{-3}}$.

In fig. 10 the map displaying the radon concentration AM for each municipality of Piemonte is reported.

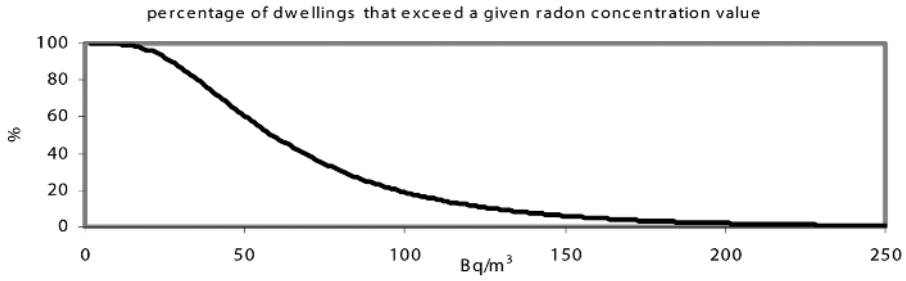

Figure 9: Estimation, by means of eq. (5) of the percentage of the dwellings of Piemonte exceeding a given radon concentration value (ground floor).

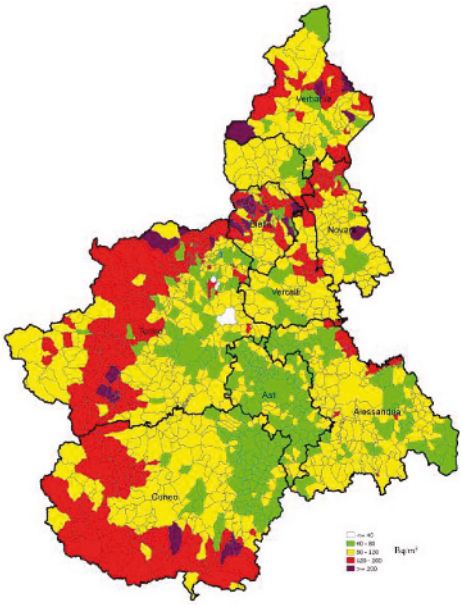

Figure 10: Average values in the municipalities of Piemonte - ground floor concentration (Bq m^{-3}).

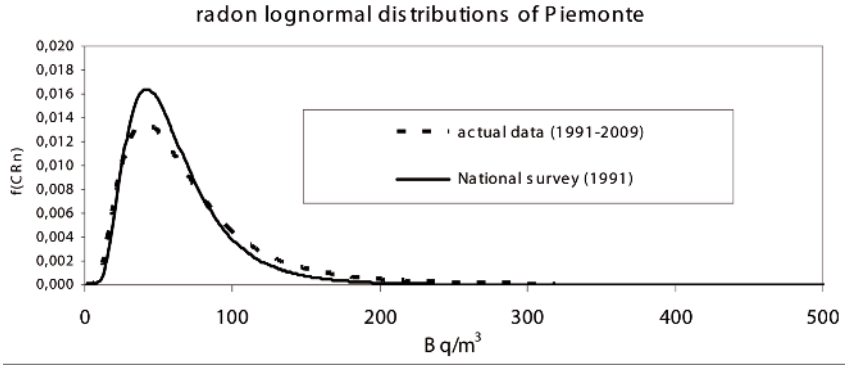

Figure 11: Distribution of the radon concentration in dwellings.

4 Conclusions

With the present work it was possible to estimate the average radon levels in each of the 1206 municipalities of Piemonte (fig. 9), more interestingly, to assess the percentage of the population exposed above a given radon concentration (fig. 10), and to define the radon prone areas of the Region, an important achievement in order to evaluate the possible health effects for the population. The overall results (Regional arithmetic mean = 71 Bq m^{-3}) were also in good agreement (fig. 11) with those obtained in the first radon survey (National survey: 69 Bq m^{-3}), performed in 1991 with a limited sampling program (430 dwellings).

Acknowledgements

We are particularly grateful to Paolo Tonanzi, Alessandra Troglia, Marina Zerbato, Anselmo Cucchi and Paolo Falletti (ARPA Piemonte) for the contribution in the geological studies, radon surveys and for the helpful comments and suggestions. We also thank Stefano Bertino, Rosa Maria Tripodi, Maura Ghione, Brunella Bellotto, and Giuliana Garbarino (ARPA Piemonte) for gamma spectrometry measurements.

References

L. TOMMASINO *et al.*, Plastic-bag sampler for passive radon monitoring, Nuclear Tracks, Vol. 12; 1986.

ISS, I rivelatori a tracce nucleari per la misura della concentrazione di radon in aria: analisi critica ed esperienze italiane a confronto, Roma 2001.

S. DARBY *et al.*, Radon in homes and risk of lung cancer: collaborative analysis of individual data from 13 European case-control studies, BMJ Volume 330; 2005.

F. BOCHICCHIO, Radon epidemiology and nuclear track detectors: methods, results and perspectives, Radiation Measurements Vol. 40, pp. 177-190; 2005.

F. BOCHICCHIO *et al.*, Annual average and seasonal variations of residential radon concentration for all the Italian Regions, Radiation Measurements, Vol. 40, pp. 686-694; 2005.

WHO-IARC. Monograph on the Evaluation of Carcinogenic Risks to Humans: Man-made mineral fibres and Radon. IARC Monograph Vol. 43, Lyon, France; 1988.

WHO Handbook on indoor radon – A public health perspective. WHO 2009.

M. MAGNONI and S. TOFANI, Indoor radon measurements in anomalous sites of Piedmont, Italy, Radiation Protection Dosimetry, Vol. 56, pp. 327-329; 1994.

Regione Veneto – ARPAV. Indagine regionale per l'individuazione delle aree ad alto potenziale radon nel territorio Veneto, Rapporto tecnico ARPAV; 2000.

P.N. PRICE *et al.*, Bayesian prediction of mean indoor radon concentrations for Minnesota counties. Health Phys. 71(6):922-936; 1996.

P.N. PRICE, Predictions and maps of country mean indoor radon concentrations in the mid-atlantic states, Health Phys. 72(6):893-906; 1997.

LSP-Sezione Fisica USSL n°40 Ivrea. Indagine sull'esposizione alla radioattività naturale nelle abitazioni del Piemonte, Regione Piemonte; 1994.

ISS-ANPA. Indagine nazionale sulla radioattività naturale nelle abitazioni, ISTISAN Congressi 34; 1994.

F. Bochicchio *et al.*, Areas with high radon levels in Italy, Proceedings of the Conference Radon in the Living Environment, 19-23 April 1999, Athens, Greece.

F. BOCHICCHIO *et al.*, Results of the representative Italian national survey on radon indoors. Health Phys. 71(5):741-748; 1996.

M. MAGNONI *et al.*, La misura dell'^{238}U mediante spettrometria gamma in matrici ambientali, Convegno Nazionale AIRP-Pisa; 2008.

E. CHIABERTO *et al.*, "Il radon in Piemonte. Dalla distribuzione delle concentrazioni alla definizione delle aree a rischio: criteri a confronto"; Proceedings of the AIRP Conference; Torino 2006.

ARPA Piemonte. La mappatura del radon in Piemonte. 2009; `www.arpa.piemonte.it`.

J. MILES and K.BALL, Mapping radon-prone areas house radon data and geological boundaries, Environ. Int. 22 (1996) S779-S782.

J. MILES, Development of maps of radon-prone areas using radon measurements in houses. 1998 NRPB – Pub. Elsevier Science.

P. BOSSEW, G. DUBOIS, T. TOLLEFSEN, Investigatios on indoor Radon in Austria, part 2: Geological classes as categorical external drift for spatial modelling of the Radon potential. Journal of Env. Radioactivity 99; 2008.

J. MILES and D. APPLETON, Mapping variation in radon potential both between and within geological units. Journal Radiation Protection 25; 2005.

L.C.S. GUNDERSEN and R.R. SCHUMANN, Mapping the radon potential of the united states: examples from the Appalachians. Environmental International Vol. 22 pp. S829-S837; 1996.

EPA map of radon zones; `www.epa.it`.